

## Apparent absence of electromagnetic or strong-interaction time-reversal violation in the decay of $^{180}\text{Hf}^m$ †

K. S. Krane

*Lawrence Berkeley Laboratory, University of California, Berkeley, California 94720*

B. T. Murdoch\* and W. A. Steyert

*Los Alamos Scientific Laboratory, P. O. Box 1663, Los Alamos, New Mexico 87544*

(Received 24 January 1974)

Time reversal ( $T$ ) invariance in the nuclear interaction was investigated by observing the directional correlation of the strongly hindered 501-keV  $\gamma$  ray of  $^{180}\text{Hf}$  with the subsequent 332- and 215-keV  $\gamma$  rays from a source of  $^{180}\text{Hf}^m$  polarized at low temperatures. The asymmetry of the correlation was measured to be  $(2.8 \pm 5.1) \times 10^{-4}$ , corresponding to a phase angle between the 501-keV  $E3$  and  $M2$  multipoles given by  $\sin\eta = 0.048 \pm 0.087$ , consistent with the assumption of  $T$  invariance. Upper limits on the out-of-phase components of the  $E3$  and  $M2$  matrix elements were determined to be  $3 \times 10^{-6}$  and  $1 \times 10^{-8}$  Weisskopf units, respectively; these extremely small upper limits result from the use of a strongly hindered  $\gamma$  ray. In addition, based on these results, estimates of the magnitude of the  $T$ -odd potential were deduced, from which we conclude that the millistrong or electromagnetic interactions are unlikely to be a source of  $T$  violations.

[ RADIOACTIVITY  $^{180}\text{Hf}^m$ ;  $\gamma$ - $\gamma$  directional correlation, time-reversal test; 501-keV  $\gamma$ , measured  $\sin\eta$ ,  $\sin\bar{\eta}$ ; deduced  $T$ -odd parts,  $E3$ ,  $M2$  transition matrices; estimated  $T$ -odd component, Hamiltonian. ]

### I. INTRODUCTION

The use of fundamental symmetries in deriving elementary conservation laws in quantum mechanical calculations is a well-known means of simplifying the equations describing physical processes. It is generally assumed that such equations can be expressed in a representation consistent with the assumption of time-reversal symmetry ( $T$ ); this is generally manifest as matrix elements and their Hermitian conjugates appearing with equal amplitudes, and leads to the conclusion that the phases of the Hamiltonian and state vectors may be chosen such that various matrix elements are relatively real. A theoretical and experimental survey of the implications of  $T$  violation is given in the work of Henley.<sup>1</sup>

A possible violation of  $T$  is suggested by the experiment of Christenson *et al.*<sup>2</sup> who observed evidence for  $CP$  (simultaneous charge conjugation and spatial parity)—violation in the decay of the long-lived neutral  $K$  meson. This implies violation of  $T$  if  $CPT$  conservation is assumed; the  $CPT$  theorem is fundamental for all processes which can be described by local field theory, and the present-day formulation of theoretical physics is such that one would prefer to maintain the validity of  $CPT$  even at the expense of  $T$ . The evidence for  $CP$  violation has prompted a number of investigations for more direct evidence for  $T$  violation, particu-

larly in nuclear  $\gamma$  decay.<sup>3-9</sup> No evidence for  $T$  violation has been found in previous studies to the limit of effects of the order of  $10^{-3}$ ; however, the use of complex nuclei for these studies introduces considerable difficulty in interpretation and necessitates rather detailed computations to attempt to separate the  $T$ -violating from the  $T$ -conserving matrix elements and to compare the former with predictions of possible  $T$ -violating Hamiltonians. In only one previous case has such a computation been attempted.<sup>10</sup>

A number of possible origins for the  $2 \times 10^{-3}$  amplitude  $CP$ -violating interaction appearing in the  $K_L^0 \rightarrow 2\pi$  decay have been suggested, which have been summarized, for example, by Blin-Stoyle.<sup>11</sup> These may be roughly classified into three groups, according to the hypercharge ( $Y$ ) selection rules they satisfy. (1)  $\Delta Y = 0$ . Here the  $T$  violation may arise from the so-called "milli-strong" interaction or else from the electromagnetic interaction itself, and effects of order  $10^{-3}$  might be expected in nuclear electromagnetic transitions. (2)  $\Delta Y = 1$ . Here the  $T$  violation is associated with weak forces, and occurs with amplitude  $10^{-3}$  relative to the weak interaction and is hence referred to as "milli-weak." Many of the milliweak models of  $CP$  violation contain a  $CP$ -violating  $\Delta Y = 0$  component as well. Thus we might expect effects in  $\gamma$  decay of order  $10^{-8}$  or  $10^{-9}$ . (3)  $\Delta Y = 2$ . Here some as yet unknown "superweak" interaction produces  $T$  vio-

lation of relative amplitude  $10^{-13}$  in  $\gamma$  decay, but cancellations give rise to an anomalously large effect in  $K_L^0$  decay, an effect of such magnitude not being expected in any other case. Clearly it is desirable to attempt experiments at the  $10^{-3}$  limit of the strong interaction in  $\gamma$  decay in order that the possibility of  $T$  violation of the type (1) above may be investigated.

In order to obtain a meaningful interpretation of the results of a  $\gamma$ -decay  $T$  experiment, one must know the extent to which the  $T$ -conserving interactions affect the laboratory observables. Here it seems advisable to choose a case for study in which the  $\gamma$  transition is greatly retarded. In this case it may be possible to obtain a relative enhancement of any  $T$ -violating component. This possibility has been recently discussed by Steyert and Krane.<sup>12</sup> The use of retarded transitions has proved effective in studies of  $P$  violation<sup>13,14</sup> and has been suggested by Clement and Heller<sup>15</sup> to be of use in studies of  $T$  violation in  $\gamma$  decay and by Barroso and Blin-Stoyle<sup>16</sup> in  $\beta$  decay. The present work reports on the first test of  $T$  violation in nuclear  $\gamma$  decay using the enhancement concept. The study was undertaken on the 501-keV transition of  $^{180}\text{Hf}$ , in which the same enhancement consideration gives rise to the largest observable case of irregular parity multipoles yet observed.<sup>13,14</sup> An abbreviated report of the present work has been given previously.<sup>17</sup>

## II. $^{180}\text{Hf}^m$ DECAY SCHEME

The decay scheme of  $^{180}\text{Hf}^m$  is shown in Fig. 1.<sup>18</sup> The 5.5-h isomer is assigned as an intrinsic excitation having eight units of spin projection on the nuclear symmetry axis ( $K=8$ ); the large value of the magnetic moment of this state [ $\mu=(8.6\pm 1.0)\mu_N$ <sup>19</sup>] identifies it as a two-proton configuration. The isomer decays to the  $8^+$  and  $6^+$  rotational states of the ground-state band ( $K=0$ ) with total branching

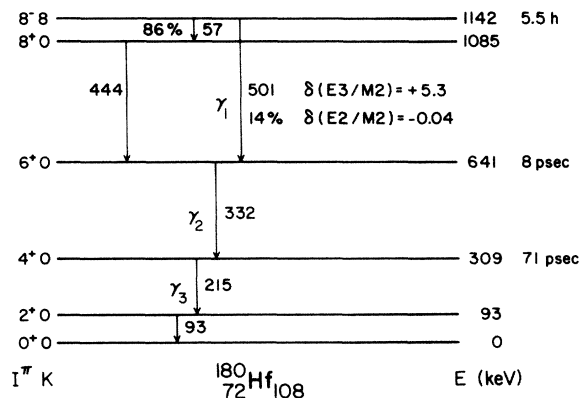


FIG. 1. Decay scheme of  $^{180}\text{Hf}^m$ .

intensities 86 and 14%, respectively. The transition of interest for the present work is the 501-keV  $\gamma$  ray, which is of mixed  $M2+E3$  multipolarity. The amplitude mixing ratio  $E3/M2$  has been measured to be +5.3.<sup>14,20</sup> The  $K$ -selection rule for  $\gamma$  transitions ( $L \geq \Delta K$ ) results in the strong retardation of the 501-keV  $\gamma$ -ray multipoles relative to single-particle Weisskopf estimates; the  $M2$  and  $E3$  transition probabilities have hindrances relative to Weisskopf estimates of  $H_w(M2) = 1.3 \times 10^{14}$  and  $H_w(E3) = 2.0 \times 10^9$  (the  $\gamma$ -ray matrix elements are reduced relative to Weisskopf estimates by the respective square roots of these numbers).

The unusually large hindrances associated with the 501-keV transition (or rather with its "regular"  $P$ - and  $T$ -conserving multipoles) may aid the observation of "irregular"  $P$ - and  $T$ -violating multipoles in the radiation field if they are not also similarly hindered. Previous studies have indeed confirmed the presence of a  $P$ -irregular  $E2$  multipole with an  $E2/M2$  amplitude mixing ratio of  $-0.04$ .<sup>13,14</sup> Although this  $E2$  multipole produces quite a substantial laboratory effect (a 1.6%  $0^\circ$ - $180^\circ$  asymmetry in the decay of polarized  $^{180}\text{Hf}^m$ ), the  $E2$  multipole is also rather strongly hindered, with  $H_w(E2) = 2 \times 10^9$ . However, here most of the hindrance is associated with the weakness (relative strength about  $10^{-6}$  or  $10^{-7}$ ) of the parity violating interaction. Thus, nuclear-structure effects provide only an additional hindrance of  $2 \times 10^2$  or  $2 \times 10^3$  in this case. It is likely that the weak interaction force responsible for the  $P$ -irregular multipoles is similar in character to that of the normal strong nuclear interaction, and thus it is not too surprising that the irregular  $\gamma$  transition is hindered by intrinsic nuclear-structure effects. However,  $T$ -violating interactions are probably not at all similar to the regular strong or weak interaction operators and thus it is extremely unlikely that the  $T$ -violating transition intensities will be similarly hindered. Thus  $^{180}\text{Hf}$  may provide a test of  $T$  violation even more sensitive than that of  $P$  violation.

In the present work we observe the angular correlation from the polarized initial level at 1142 keV between the mixed  $E3+M2$  501-keV  $\gamma$  ray and either the subsequent pure  $E2$  332- or 215-keV  $\gamma$  rays. Since the sequence of transitions depopulating the  $6^+$  level constitutes a basic sequence, the 332- and 215-keV transitions have identical angular correlations (neglecting perturbations) in coincidence with the 501-keV transition.

## III. THEORY OF THE METHOD

The various observables necessary to test  $T$  invariance in  $\gamma$  decay, all of which involve a search

for interference between the  $L$  and  $L+1$  multipole components in the radiation field, have been summarized by Jacobsohn and Henley<sup>21</sup> and by Boehm.<sup>22</sup> The effect of the  $T$  violation is to negate the assumption that the phases can be chosen so that the multipole matrix elements are relatively real, and the amplitude mixing ratio of the  $L+1$  and  $L$  components becomes complex, characterized by the phase angle  $\eta$ , as

$$\delta = |\delta| e^{i\eta}. \quad (1)$$

One of the possible tests involves the measurement of the scalar quantity  $\langle (\vec{I} \cdot \vec{k} \times \vec{k}') (\vec{k} \cdot \vec{k}') \rangle$ . Here  $\vec{I}$  represents the nuclear polarization,  $\vec{k}$  represents the momentum of the mixed-multipole  $\gamma$  ray, and  $\vec{k}'$  represents the momentum of a subsequent (cascade)  $\gamma$  ray. The measurement thus involves a  $\gamma$ - $\gamma$  directional correlation from a polarized initial state. The general theory for such correlations has been recently described by Krane, Steffen, and Wheeler,<sup>23</sup> and the relevant details will

be briefly summarized here. The polarization axis is chosen as the  $z$  axis,  $\theta_1$  and  $\theta_2$  describe, respectively, the polar angles of emission of  $\gamma_1$  and  $\gamma_2$  with respect to  $z$ , and  $\phi$  gives the azimuthal angle between the  $(\gamma_1 z)$  and  $(\gamma_2 z)$  planes. The directional correlation may then be written as

$$W(\theta_1, \theta_2, \phi) = \sum_{\lambda_1 \lambda_2} Q_{\lambda_1}(\gamma_1) Q_{\lambda_2}(\gamma_2) B_{\lambda_1}(\eta) A_{\lambda_2}^{\lambda_2 \lambda_1}(\gamma_1) \times A_{\lambda_2}(\gamma_2) H_{\lambda_1 \lambda_2}(\theta_1, \theta_2, \phi). \quad (2)$$

The orientation parameters  $B_{\lambda_1}$ , the angular distribution parameters  $A_{\lambda_2}$  of the second  $\gamma$  ray, and the solid-angle correction factors  $Q_{\lambda_1}$  and  $Q_{\lambda_2}$  are identical with those generally employed in angular distribution and correlation studies. The generalized angular distribution coefficient  $A_{\lambda_2}^{\lambda_2 \lambda_1}(\gamma_1)$  for

$$I_i \xrightarrow{\gamma_1} I_f$$

is given for  $T$  even ( $\lambda_1 + \lambda_2 = \text{even}$ ) by

$$A_{\lambda_2}^{\lambda_2 \lambda_1} = \frac{F_{\lambda_2}^{\lambda_2 \lambda_1}(LL'I_f I_i) + 2|\delta| \cos \eta F_{\lambda_2}^{\lambda_2 \lambda_1}(LL'I_f I_i) + |\delta|^2 F_{\lambda_2}^{\lambda_2 \lambda_1}(L'L'I_f I_i)}{1 + |\delta|^2} \quad (3a)$$

and for  $T$  odd ( $\lambda_1 + \lambda_2 = \text{odd}$ ) by

$$A_{\lambda_2}^{\lambda_2 \lambda_1} = \frac{2i|\delta| \sin \eta}{1 + |\delta|^2} F_{\lambda_2}^{\lambda_2 \lambda_1}(LL'I_f I_i), \quad (3b)$$

where  $\delta$  is the  $\gamma$ -ray mixing ratio in the phase convention of Krane and Steffen.<sup>24</sup> The generalized  $F$  coefficients  $F_{\lambda_2}^{\lambda_2 \lambda_1}$  have been tabulated for cases relevant to  $T$ -violation studies by Krane.<sup>25</sup>

The angular function  $H_{\lambda_1 \lambda_2}$  is given by<sup>23</sup>

$$H_{\lambda_1 \lambda_2}(\theta_1, \theta_2, \phi) = \sum_{q \geq 0} \begin{Bmatrix} 2 - \delta_{q0} \\ -2i \end{Bmatrix} \langle \lambda_1 0 \lambda q | \lambda_2 q \rangle (-1)^q \times \left( \frac{2\lambda + 1}{2\lambda_2 + 1} \right)^{1/2} \left[ \frac{(\lambda - q)! (\lambda_2 - q)!}{(\lambda + q)! (\lambda_2 + q)!} \right]^{1/2} \times P_{\lambda}^q(\cos \theta_1) P_{\lambda_2}^q(\cos \theta_2) \begin{Bmatrix} \cos q \phi \\ \sin q \phi \end{Bmatrix}. \quad (4)$$

Of the two pairs of quantities in braces, the upper member refers to cases in which  $\lambda_1 + \lambda_2$  is even, while the lower member is for odd values of that sum; the latter case is the one of interest for studies of time-reversal invariance. The  $P_{\lambda}^q$  are the associated Legendre polynomials.

For directional  $\gamma$ -ray distributions (no polarizations are measured),  $\lambda$  and  $\lambda_2$  are restricted to even values, and hence  $\lambda_1$  must be odd for studies

of  $T$  violation (i.e., the initial state must be polarized).

The angular distribution may then be written as

$$W = W_0 + W_T + W', \quad (5)$$

where  $W_0$  and  $W_T$  contain the  $T$ -conserving and  $T$ -violating terms (or, equivalently, the  $\lambda_1 = \text{even}$  and  $\lambda_1 = \text{odd}$  terms), respectively. An additional term  $W'$  has been included to account for possible polarization-sensitive  $T$ -nonviolating effects discussed below. By periodically reversing the direction of nuclear polarization we compute the asymmetry  $\alpha$ , defined by

$$\alpha = \frac{W(\uparrow) - W(\downarrow)}{W(\uparrow) + W(\downarrow)}. \quad (6)$$

$W(\uparrow)$  and  $W(\downarrow)$  indicate the measured correlation with nuclear spin up and down, respectively. Since the  $\lambda_1$ -odd terms in  $W_T$  change sign under this reversal while the  $\lambda_1$ -even terms in  $W_0$  do not, this may be written, assuming  $W_T \ll W_0$ , as

$$\alpha \approx \frac{W_T + W'}{W_0}. \quad (7)$$

At a temperature of 20 mK,  $W_0 = 1.297$ , for both the 501-332- and 501-(332)-215 keV cascades, while the lowest-order nonzero ( $\lambda_1 = 1$ ,  $\lambda = \lambda_2 = 2$ )  $T$ -violating term, corresponding to

$$\langle (\vec{I} \cdot \vec{k} \times \vec{k}') (\vec{k} \cdot \vec{k}') \rangle,$$

is given for either case by

$$W_T = Q_2(\gamma_1)Q_2(\gamma_2)B_1F_2^{21}(\gamma_1) \times \frac{2|\delta| \sin\eta}{1+|\delta|^2} F_2(\gamma_2)(-0.6124 \sin 2\phi), \quad (8)$$

where  $\delta$  is the 501-keV mixing ratio. Inserting the appropriate factors, and including the higher-order terms which cancel roughly one-third the magnitude of the above expression for  $W_T$ , we obtain

$$W_T = +0.0076 \sin\eta. \quad (9)$$

It should be noted that the summation over the  $\lambda$ 's in Eq. (2) is equivalent to the simultaneous measurement of the observables corresponding to a number of vector products, although the dominant contribution is that given by Eq. (8). The geometry is chosen such as to maximize any effect arising from this term; however, all of the vector products contain the vectors  $\hat{I}$ ,  $\hat{k}$ , and  $\hat{k}'$  *in toto* an odd number of times, and hence all are odd with respect to  $T$ . Thus the measurement of any nonvanishing correlation of the form of  $W_T$  is sufficient to establish the presence of  $T$  violation. It should also be noted that lower-order correlations of the form  $\hat{I} \cdot \hat{k} \times \hat{k}'$  may also be observed; this form has been suggested, for example, by Blin-Stoyle.<sup>11</sup> Such a correlation requires the presence of either parity violation or circular polarization detection efficiency in both  $\gamma_1$  and  $\gamma_2$ . Although  $\gamma_1$  does indeed contain a parity-violating multipole (of order  $10^{-2}$ ), it is not expected that  $\gamma_2$  does likewise; furthermore, we estimate the sensitivity of our system to the circular polarization of  $\gamma_2$  to be less than  $10^{-4}$ . Thus such correlations are not expected to contribute above the  $10^{-6}$  level which is beyond the scope of the present work.

The effect of temperature variation on the values of  $W_0$  and  $W_T$  is small (about 1% per mK in  $W_0$  and about 0.2% per mK in  $W_T$ ). The small variation in  $W_0$  arises from the lack of cancellation among the leading order terms (those proportional to  $B_0$ ) in  $W_0$ ; it is these identical terms which result in the isotropy of the directional correlation when the initial state is random.<sup>20</sup> The small variation in  $W_T$  results from cancellation between the temperature variations of the  $B_1$  and  $B_3$  terms.

The quantity  $W'$  included in the expression for  $W$  signifies polarization-sensitive effects which simulate  $T$  violation. For the present case, these may be ascribed to two causes, such that

$$W' = W'_{\text{PAC}} + W'_{\text{PV}}. \quad (10)$$

The asymmetry  $W'_{\text{PAC}}$  results from precession of the intermediate state due to the perturbation

of the angular correlation by magnetic hyperfine interactions.<sup>26</sup> This effect results in an azimuthal shift  $\Delta\phi$  which may be computed from the known hyperfine field of Hf in  $\text{ZrFe}_2$  and from the  $g_R$  factor of the  $^{180}\text{Hf}$  ground-state rotational band ( $g_R = 0.26$ ),<sup>27</sup> resulting in

$$\begin{aligned} \Delta\phi(6^+) &= -0.2^\circ, \\ \Delta\phi(4^+) &= -1.5^\circ. \end{aligned} \quad (11)$$

The negative sign indicates that the correlation pattern shifts toward smaller values of  $\phi$ , and thus the effective value of  $\phi$  is slightly larger than  $\frac{3}{4}\pi$ . Such an azimuthal shift introduces a spurious asymmetry which can be computed as

$$\begin{aligned} W'_{\text{PAC}}(\gamma_1 - \gamma_2) &= +0.4 \times 10^{-4}, \\ W'_{\text{PAC}}(\gamma_1 - \gamma_3) &= +3.3 \times 10^{-4}. \end{aligned} \quad (12)$$

The uncertainties of these values are about 10%, resulting from the uncertainties in the 501-keV mixing ratio. It should be noted that the small magnitude of this correction is a fortuitous result of the isotropy of the angular correlation from the random initial state.<sup>20</sup>

The effect of  $W'_{\text{PV}}$  results from the rather large asymmetry of the 501-keV  $\gamma$  ray due to parity mixing in the  $8^-$  level.<sup>14</sup> This effect would vanish if  $\theta_1$  were exactly equal to  $\frac{1}{2}\pi$ , and hence small misalignments of the detectors produce this effect. A measure of the magnitude of  $W'_{\text{PV}}$  may be obtained from the value of the asymmetry  $\mathcal{G}_{501}$  computed according to Eq. (6) for the 501-keV  $\gamma$ -ray singles counting rates; this asymmetry should likewise vanish for  $\theta_1 = \frac{1}{2}\pi$ . The effect of this perturbation on the angular correlation is computed to be

$$W'_{\text{PV}} = 1.8\mathcal{G}_{501}. \quad (13)$$

#### IV. EXPERIMENTAL DETAILS

##### A. Sample preparation

As in the measurements of parity nonconservation in the  $\gamma$  decay of  $^{180}\text{Hf}^m$ ,<sup>14</sup> the Hf was arc-melted with Zr and Fe to form the cubic ferromagnet  $(\text{Hf}_{0.05}\text{Zr}_{0.95})\text{Fe}_2$ . Crystal bar Hf enriched in  $^{179}\text{Hf}$  was used (87%  $^{179}\text{Hf}$ , 8.5%  $^{180}\text{Hf}$ , 3.3%  $^{178}\text{Hf}$ , 1%  $^{177}\text{Hf}$ , 0.2%  $^{176}\text{Hf}$ ) in order to minimize contamination with  $^{181}\text{Hf}$  decay  $\gamma$  rays. In  $\text{ZrFe}_2$ , Hf experiences a magnetic hyperfine field of  $-200 \pm 20$  kOe, resulting in an energy difference  $\Delta = \mu H/I$  between the adjacent magnetic hyperfine levels (corresponding to different values of  $I_z$ ) of the  $8^-$  state of  $-7.9 \pm 0.5$  mK. At dilution refrigerator temperatures of 20 to 35 mK, polarizations approaching unity are achieved. The nuclei align in a direction which is opposite to that of the  $(\text{Hf}, \text{Zr})\text{Fe}_2$  polarization. The  $(\text{Hf}, \text{Zr})\text{Fe}_2$  polar-

ization is in turn parallel to the direction of the modest magnetic field applied to polarize the ferromagnet (in these experiments, a generous 5 kOe was used). Thus, the nuclear polarization is opposite to the applied magnetic field.

For ease of polarization, and in order to minimize  $\gamma$ -ray absorption, the samples (after annealing at 950°C for 16 h) were cut into 7-mm  $\times$  1-mm  $\times$  1-mm needles and were activated in the Los Alamos Omega West Reactor, receiving total integrated fluxes of  $4 \times 10^{15}$  neutrons/cm<sup>2</sup>. They were mounted and polarized vertically in the cryostat, while the detectors observed  $\gamma$  rays emitted normal to the long vertical sample axis.

#### B. Cryogenic apparatus

Figure 2 shows the cryogenic assembly. The sample is soldered with high purity indium onto a copper fin, the upper end of which is threaded. This is inserted through the bottom of the refrigerator vacuum can and screws into a split copper receptacle which is in turn indium-soldered to the cold finger coming down from the mixing chamber of the <sup>3</sup>He-<sup>4</sup>He dilution refrigerator. Adequate thermal contact is provided from the sample to the refrigerator: (1) through the indium solder which is driven normal by the high applied field, (2) through the copper-to-copper screw joint which is very tight at low temperatures because of contraction in the nylon collar, and finally (3) through

the cold finger. The cold finger is fabricated from 15 0.04-cm diam high purity annealed copper wires spot-welded to the mixing chamber which contains a sintered copper disk for thermal contact to the mixture. Electrical resistance at liquid N<sub>2</sub> temperature across this screw joint was measured as 7  $\mu\Omega$ . This design is predicated on requirements of good thermal contact, minimization of eddy current heating due to the periodic magnetic field reversals, and convenience of sample changing. The time involved in inserting the sample, soldering the 1.3-cm cap on the bottom of the refrigerator vacuum bulb, replacing the He and N<sub>2</sub> Dewars, and cooling to 35 mK is about 6 h. The operating temperature of the refrigerator mixing chamber in the absence of any heat load is 14 mK.

Also schematically shown in Fig. 2 are the vertical superconducting magnets which were used to provide the vertical polarizing field on the sample. They were 2 cm in diameter with 1.8 cm separating the two coils of 1000 turns each. The field at the sample was 0.54 kOe per ampere. The horizontal coils, 2 cm in diameter and 2.5 cm apart had 500 turns each and provided 0.1 kOe per ampere. Both sets of coils were fabricated from 0.013-cm diam Supercon<sup>28</sup> type T48B Formvar insulated copper-clad NbTi wire. The current leads from the magnet power supply were 0.05-cm diam copper-clad NbTi wire.

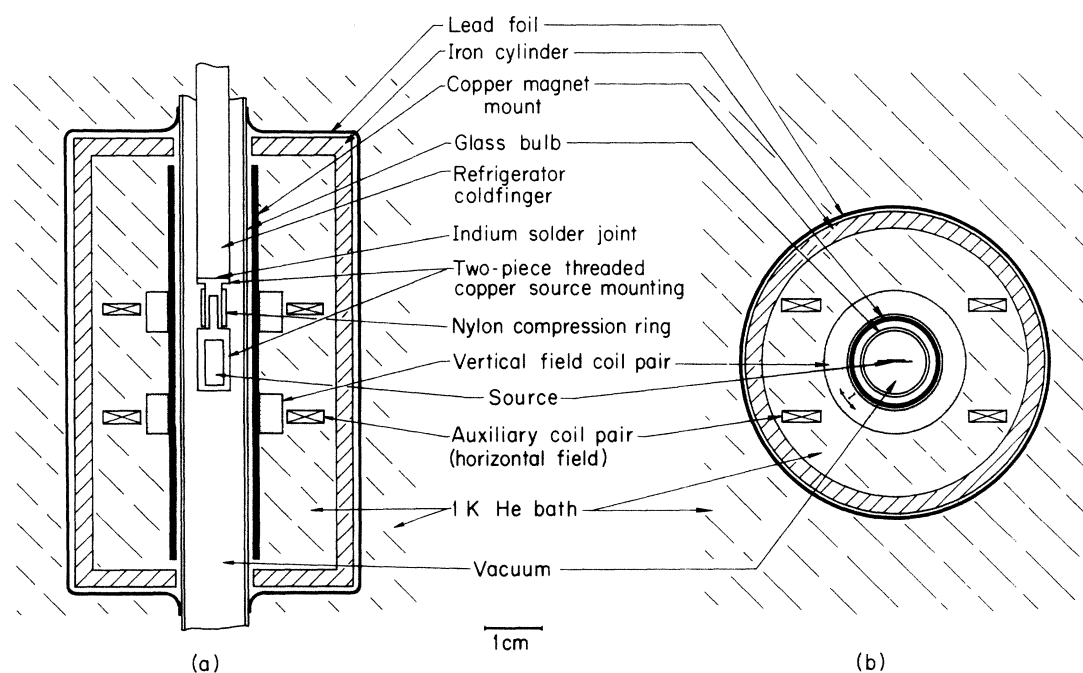


FIG. 2. Schematic representation of interior of cryostat, showing source mounting arrangement, polarizing coils, magnetic shielding, and a portion of the cryogenics.

To reverse the nuclear polarization, the magnetic field is rotated by gradually turning on the horizontal coils while the vertical coils are gradually being turned off. When the vertical coil current is zero, the leads are reversed via a double-pole-double-throw relay, and the vertical coils are again gradually energized while the  $90^\circ$  coils are gradually turned off. Each  $90^\circ$  rotation takes 20 sec. Because the magnetic field is rotated rather than reversed magnetic hysteresis energy dissipation is much smaller. Also the nuclei are able to follow the slowly rotating field, and no nuclear relaxation is required before the nuclei assume their new opposite polarization (nuclear spin lattice relaxation times at these temperatures are typically many seconds). Many of these cryogenic considerations are discussed in further detail in Ref. 29.

### C. Electronics

Data are accumulated in and the experiment is controlled by a Nova<sup>30</sup> minicomputer-based data acquisition system<sup>31</sup> which is shown in Fig. 3. With the aid of the block diagram in Fig. 3 and the

coincidence and singles pulse height spectra shown in Fig. 4, we can discuss the types of data which are accumulated by the system. The detector pulses are digitized by the analog-to-digital converters (ADC's) and through the data channel the appropriate memory location in the computer is incremented. However, in order to keep the ADC dead time small ( $\approx 10\%$ ) only 1 in 10 singles pulses is stored (the ADC's are operated such as to require a logic pulse into the coincidence input to digitize the pulse). But if the other detector registers a pulse from the particular peak of interest (501 keV) in coincidence (resolving time  $2\tau = 0.8 \mu\text{sec}$ ) with this pulse, the pulse is always digitized and it is stored in a different memory location to form the coincidence spectrum.

The computer records the number of seconds that the ADC has been alive for the preset real-time counting period. It also records the number of times that the "particular peak" (501 keV) timing single-channel analyzers (SCA's) have been triggered. At the end of the preset counting period, and while the nuclear polarization is being rotated, the computer calculates the required counting

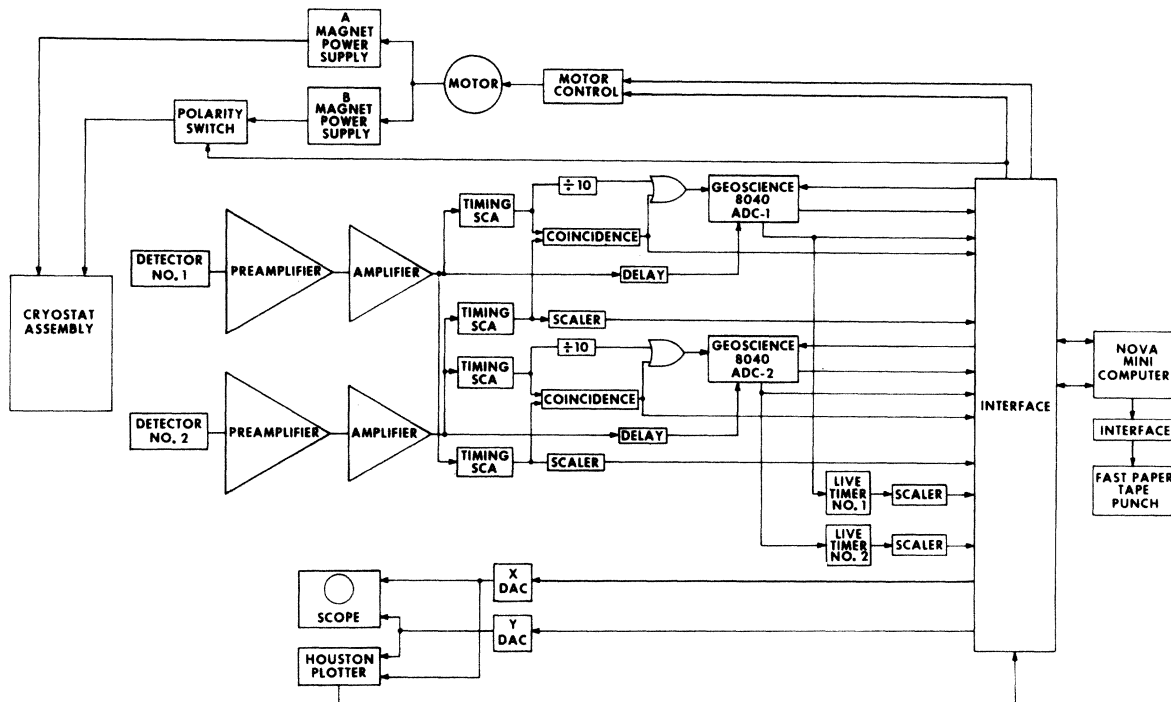


FIG. 3. Block diagram of electronics. Computer controls magnet currents and polarity of vertical (B) coils. Linear signals into the ADC's are gated by coincidence and every 10th singles pulse. Digitized pulse height information (when gated) increments a memory location in a computer memory block determined by the presence or absence of a coincidence signal. The computer turns the ADC's on and off. Scalers, fed by the timing SCA's which are set on the 501-keV peak, monitor these SCA's output rate. The divide-by-10 circuits are fed by SCA's set on the entire spectrum. The spectra can be monitored on a scope or plotter; the horizontal (x) signal is used to turn the plotter on and off. The plotter signals the computer when it has completed each point plot.

rates. Knowing the approximate position of a peak of interest, it will calculate the centroid to the nearest 1/10 channel and add up the counts in a preset number of channels above and below that center. It will also add  $\frac{1}{2}$  the number of counts in a preset number of channels further away from the center (this avoids a sharp cutoff, and the arbitrariness of giving one channel full weight and the one next to it zero weight). The total number of counts calculated in this way is then divided by the live time to form the counting rate. Backgrounds in a particular region of the spectrum are also integrated. For four of the peaks the computer calculates at the end of a series for field-up and for field-down runs the exact average center of the peak to the nearest 1/100 of a channel. Any systematic gain changes with field direction would be readily apparent from these numbers. With the magnetic field directed upward, for example, data are accumulated for a preset period of time  $\tau$ , typically 5 to 20 min, following which the computer turns off the ADC's and the monitor scalers, sends out a magnet power supply motor control command to gradually turn on the horizontal magnets (magnet power supply A in Fig. 3), outputs the requested data on the tape, reverses the polarity switch, and turns supply A off and supply B (vertical coils) back on, so that current now flows in the opposite direction. This process continues automatically until manually stopped. After the third such computer period, the computer compares the results of a particular counting period, for example, the second period when the field was pointed downward, with the average counting rate of the previous and following counting period when the field was directed upward. It outputs, on paper tape, the difference and the square of this difference. As the data series progresses, the differences and their squares for the field down  $\Delta_D$  (and similarly for the field up) periods are summed as they are accumulated. When the series is manual-

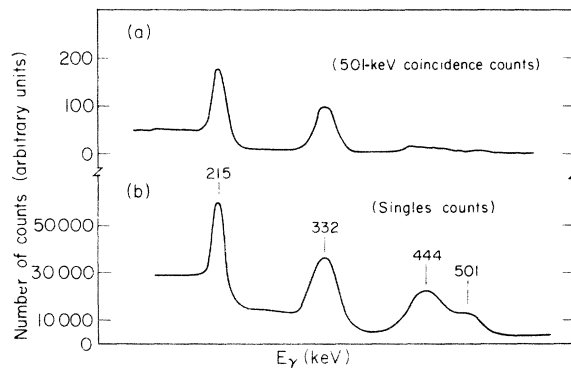


FIG. 4. Single  $\gamma$ -ray spectrum and 501-keV gated coincidence spectrum.

ly terminated after  $n$  such  $\Delta_D$ 's have been obtained, the computer calculates and outputs the raw asymmetry  $\mathcal{Q}_r$ , the average difference in a particular counting rate for field up or down divided by twice the mean counting rate  $C$ .

$$\mathcal{Q}_r = \frac{\sum \Delta_D}{2nC}. \quad (14)$$

The computer also prints out the experimental uncertainty in  $\mathcal{Q}_r$ ,  $\delta_r$ .

$$\delta_r = \frac{\sqrt{\frac{3}{2}}}{\sqrt{C\tau n}}. \quad (15)$$

The  $\sqrt{\frac{3}{2}}$  comes from the fact that each  $\Delta_D$  is the difference between one number and the average of two other numbers with the same uncertainty which are counted twice in the sequence. The computer also puts out the normalized  $\chi^2$  for the data

$$\chi^2 = \frac{\sum (\Delta_D - \bar{\Delta}_D)^2 \tau^2}{\frac{3}{2} C \tau (n-1)}. \quad (16)$$

The  $\tau^2$  in the numerator makes the numerator the sum of the squares of the fluctuations in the counts, and the denominator is the expected squared fluctuation in each  $\Delta_D$  times  $n-1$  (required to make the expected  $\chi^2 = 1$ ).

#### D. Detector configuration

For this experiment two 7.6-cm  $\times$  7.6-cm NaI(Tl) detectors mounted on the Dewar were used to provide high photopeak efficiency  $\epsilon$  for the coincidence experiments. The upper limit on the source strength and counting rate was imposed by detector pulse pileup considerations rather than by cryo-

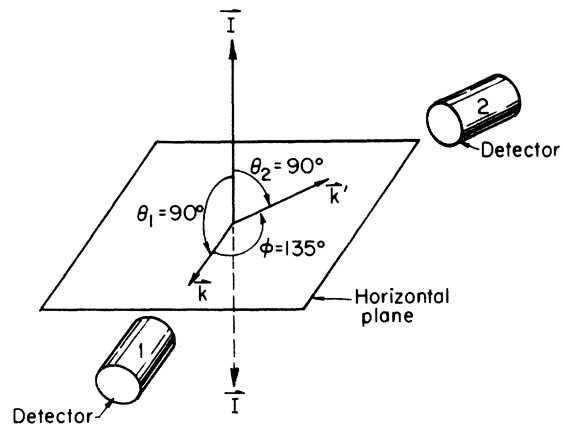


FIG. 5. Geometrical relationship between polarization axis and detection position.  $\vec{I}$  represents the direction of nuclear polarization, and  $\vec{k}$  and  $\vec{k}'$  represent the momenta of the  $\gamma$  rays. The azimuthal angle  $\phi$  is always measured from the direction of  $\gamma_1$  in a right-hand sense referenced to the polarization axis.

genic or coincidence true-to-accidental considerations.

The  $135^\circ$  interdetector angle was chosen so as to maximize the magnitude of the scalar

$$(\vec{I} \cdot \vec{k} \times \vec{k}')(\vec{k} \cdot \vec{k}')$$

(at  $45^\circ$  the detectors are too close together to fit conveniently, and detector-to-detector  $\gamma$  scattering could be a problem). The geometry is shown schematically in Fig. 5. The detector distance is a compromise between the requirements for a high-coincidence counting rate (which goes like product of the two detector efficiencies) and the need to keep the solid angle correction factor  $Q_2$  near unity (the  $T$ -odd effect is decreased by the product of the two detector  $Q_2$ 's). When the source was strong, the detector distance was 7–9 cm,  $\epsilon$  was about 0.03, and  $Q_2$  was about 0.85 for  $\gamma$ 's in the range of interest. As the source decayed and the detectors were moved to within 4.2 cm from the source,  $\epsilon$  grew to about 0.08 and  $Q_2$  fell to about 0.7.

The superconducting coils provide a 5-kOe field at the sample, and to prevent this fringing field from causing a systematic gain shift, sensitive to field direction, which would provide a false asymmetry in the counting rate of the 501-keV  $\gamma$  ray in the timing SCA, extensive shielding was required. First, the coils were surrounded by a soft-iron cylindrical shell 8 cm long, 5 cm in diameter, with 3-mm walls. The ends of the cylinder were almost closed as well (see Fig. 2). Even with shielding wrapped around the outside of the Dewar, and with standard magnetic shields on the detectors, field-sensitive gain shifts and SCA counting rate changes were observed. This problem was solved by the addition of a thin (0.005 cm) lead foil enclosure around the iron cylinder. This superconducting shield, soldered together with superconducting indium, prevented the escape of any stray field which would penetrate the iron except at the 2-cm-diam openings at the ends where the refrigerator sample tube entered. No stray fields in excess of 0.01 Oe were measured outside the Dewar. With the lead shielding in place, no gain or count rate changes correlated with field direction were observed to precisions of 1/5000 and 1/3000, respectively.

#### E. Evaluation of experimental method

This  $T$ -invariance test is designed to be a "difference" experiment, looking for differences in counting rates with the nuclear spins pointed up compared to when they are pointed down. Obviously this simple method eliminates some sources of error, but can cause some problems as well. The prime advantage of this method is that the experiment looks for counting rate differences with no changes in the source or detector positions, and no changes in the electronics. The difference technique not only searched for small asymmetries upon field reversal, but also accumulated simultaneous gated coincidence spectra accepting the 501-keV  $\gamma$  ray in either detector 1 or detector 2 (see Fig. 3). This symmetric detector method is equivalent to observing the correlation at  $\phi$  and  $2\pi - \phi$ , and referring to Eq. (3) we see that  $W_0(\phi) = W_0(2\pi - \phi)$ , while  $W_T(\phi) = -W_T(2\pi - \phi)$ . A similar transformation  $\phi \rightarrow 2\pi - \phi$  results from reversing the field direction (dashed line in Fig. 5). The source and detectors are rigidly mounted so as not to be moved by magnetic forces (which should not change with field reversal in any event, since the force is proportional to  $H^2$  on nonpermanent magnets). Elaborate shielding previously described prevents a magnetic field influence on the experiment. Effects of drifts in the electronics are averaged out by frequent field direction changes (every 5 min at high count rates, every 20 min at low count rates). Most sources of systematic error can be examined with the source at or above 1 K where there would be no nuclear polarization and therefore no  $T$ -odd effect. Tests for systematic error in the higher counting rate parity violation tests carried out with this equipment show no problems above the  $10^{-4}$  level.

There are, however, some cryogenic problems associated with this difference experiment technique. Each field rotation puts a few ergs of heat into the sample, primarily through magnetic hysteresis heating, and tests have shown that a continuous rotation of 0.05 Hz causes a 5 mK increase in source temperature. A field reversal instead of rotation would be intolerable. The twisted high purity (99.999%) copper wires in our refrigerator system can handle 0.6 erg/sec for  $\Delta T = 1$  mK

TABLE I. Some raw measured asymmetries ( $\times 10^4$ ).

| $E_\gamma$ (keV)       | Singles peaks |                |               |               | Coincidence peaks<br>(w/501 keV) |                |                 |
|------------------------|---------------|----------------|---------------|---------------|----------------------------------|----------------|-----------------|
|                        | 215           | 332            | 444           | 501           | 215                              | 332            | 444             |
| $T = 20\text{--}35$ mK | $0.9 \pm 0.5$ | $0.3 \pm 0.6$  | $0.6 \pm 0.6$ | $0.1 \pm 0.9$ | $7.6 \pm 4.3$                    | $0.0 \pm 4.8$  | $-1.3 \pm 8.9$  |
| $T \geq 2$ K           | $0.9 \pm 0.8$ | $-0.6 \pm 0.9$ | $1.5 \pm 1.0$ | $2.6 \pm 1.7$ | $4.7 \pm 5.9$                    | $-1.9 \pm 6.3$ | $10.4 \pm 10.0$ |



(there are 15 wires, 0.04 cm in diameter).

Another aspect of the rotating field method is the problem of nuclear phase lags between the field rotation and the nuclear rotation; this is found to be 1 sec for  $^{60}\text{Co}$  in Fe compared to 1 min for the nuclear spin lattice relaxation times. Thus, the nuclei are found to follow the nuclear rotation very nearly adiabatically.<sup>29</sup>

## V. RESULTS

The raw experimentally measured asymmetries for various singles and coincidence peaks are listed in Table I, after being averaged appropriately for both analyzer systems (see Fig. 3). Several experimental corrections were made to the 215- and 332-keV coincidence peaks as follows, in decreasing order of importance: (1) The effect of a small systematic residual asymmetry, as measured in the 501-keV singles peak and in the single-channel-analyzers set for that  $\gamma$  ray, was removed by an additive factor determined to be  $(1.4 \pm 0.9) \times 10^{-4}$  for the warm data and  $(1.7 \pm 0.5) \times 10^{-4}$  for the cold. However, as discussed above, these factors were first multiplied by a factor of 1.4 to allow for a possible parity-violating contribution from misalignment of the source and other errors. We choose a factor less than the value 1.8 previously calculated, since previously the residual effect had been assumed to be purely from misalignment, whereas we feel that misalignment is unlikely to be the sole contributor to the residual asymmetry. (2) A 15% upward correction was made to compensate for a representative true-to-chance coincidence ratio of 6.5. This ratio was found by statistically weighing periodically monitored true-to-chance measurements taken during the experiment. (3) The asymmetry in a background region lying just above the 501-keV peak in the coincidence spectrum was measured and an appropriate correction, less than 10% upward for each of the asymmetries of interest, was performed.

The 215-, 444-, and 332-keV singles peak asymmetries served as monitors of systematic problems.

After these systematic corrections were performed, the warm and cold asymmetries used in the remaining discussion were as listed in Table II.

TABLE II. Corrected experimental asymmetries ( $\times 10^4$ ).

| $E_\gamma$ (keV) | Coincidence peaks<br>(w/501 keV) |                |
|------------------|----------------------------------|----------------|
|                  | 215                              | 332            |
| $T = 20-35$ mK   | $+12.0 \pm 5.5$                  | $+2.8 \pm 6.1$ |
| $T \geq 2$ K     | $+9.1 \pm 7.6$                   | $+0.9 \pm 7.9$ |

As discussed in a previous section, a nonnegligible but uncertain amount of precession effect is expected to appear in the 501-215-keV asymmetry. In order to remove most of this effect, the warm asymmetry was subtracted from the cold to obtain the resultant value  $(2.9 \pm 9.4) \times 10^{-4}$ . This value was then averaged with the low temperature asymmetry for the 501-332-keV correlation to obtain the over-all asymmetry  $\mathcal{G} = W_\tau/W_0$  from Eq. (7)

$$\mathcal{G} = (+2.8 \pm 5.1) \times 10^{-4}.$$

With  $W_0 = 1.297$  and using Eq. (9) for  $W_\tau$  we get

$$\sin\eta = +0.048 \pm 0.087.$$

## VI. COMPARISON WITH PREVIOUS RESULTS

Similar investigations of possible  $T$  violation in  $\gamma$  radiation have been performed previously on a number of different isotopes<sup>3-9</sup>; these are summarized together with the present results in Table III. All previous experimental studies have been done on mixed  $E2/M1$  transitions; the present work uses a mixed  $E3/M2$  transition. Although the upper limit of  $\sin\eta$  deduced in the present work is somewhat larger than that of previous studies, the large hindrances of the  $\gamma$ -ray transition probabilities of the present work result in a greater sensitivity to any possible out-of-phase contribution to the multipole matrix elements. Although the absolute hindrances in many of the previous studies are unknown, the relative hindrances of the  $E2$  and  $M1$  components may be determined from the  $E2/M1$  mixing ratios, and the  $E2$  component may be assumed to be enhanced by roughly a factor of 10 in accordance with the systematic behavior of  $E2$  transitions.

The phase angle  $\eta$  which characterizes the  $T$  violation is given by (assuming  $\sin\eta$  to be small)

$$\sin\eta = \frac{1}{|\delta|} \text{Im}(\delta) \approx \frac{\text{Im}\langle L+1 \rangle}{|\langle L+1 \rangle|} - \frac{\text{Im}\langle L \rangle}{|\langle L \rangle|}. \quad (17)$$

In order to obtain meaningful relative comparisons of the matrix elements it is necessary to normalize with respect to density of final state effects (essentially energy dependence), effects of the radiation field at the origin ( $L$  dependence), and nuclear size effects ( $A$  dependence). This can be most conveniently done by expressing the matrix elements in Weisskopf units, denoted by the subscript  $W$ . We then obtain, choosing  $\langle L+1 \rangle$  to be real,

$$|\text{Im}\langle L \rangle_W| = \frac{|\langle L \rangle \sin\eta|}{\langle L \rangle_W} = |\sin\eta| [H_W(L)]^{-1/2}, \quad (18)$$

where  $H_w$  denotes the Weisskopf hindrance of the transition probability. Thus  $|\text{Im}\langle M2 \rangle_w| = (4.2 \pm 7.5) \times 10^{-9}$ . A similar expression may be obtained for  $\text{Im}\langle L+1 \rangle_w$ , assuming  $\langle L \rangle$  to be real. We obtain  $|\text{Im}\langle E3 \rangle_w| = (1.1 \pm 1.9) \times 10^{-6}$ . The results for the out-of-phase components for this and previous experiments are shown in Table III. We have used a value of  $\sin\eta$  for each case corresponding to the upper limit allowed by the experimental uncertainty; the deduced results thus represent the upper limits on the out-of-phase matrix elements permitted by each investigation. The large hindrances of the transition used in the present work yield an upper limit for the matrix elements some four orders of magnitude smaller than the best previous results.

The question remains as to whether this small upper limit of the  $T$ -odd  $\gamma$ -ray matrix element results from a hindrance of the  $T$ -odd operators in a manner similar to that of the  $T$ -even operators, or whether it results from the intrinsically small strength of the  $T$ -odd Hamiltonian. As discussed in Sec. II, nuclear structure effects probably do not strongly hinder the  $P$ -odd matrix element. Since the  $P$ -odd operators are likely to be of a two-body nature, as are the  $P$ -even operators, only a modest net enhancement is obtained. However, the  $T$ -odd nucleon-nucleon interactions may be of a three-body character,<sup>15</sup> and at very least are momentum-dependent, so that transition operators associated with such interactions are unlikely to be hindered in a manner similar to those associated with the  $T$ -even interactions. Similarly, if  $T$  violation arises in the electromagnetic field itself (as opposed to in the nuclear Hamiltonian), the  $T$ -odd transition operators will be two-body, while normal transition operators are one body. Again the  $T$ -odd matrix elements may not be hin-

dered as much as are the  $T$ -even matrix elements. We therefore conclude that, in the absence of detailed calculations of  $T$ -odd matrix elements, the hindrance concept is expected to be at least as effective in the  $T$ -odd case as in the  $P$ -odd case, and that the above-deduced out-of-phase matrix elements are probably not strongly hindered by nuclear-structure effects, but rather represent a measure of the strength of the  $T$ -odd potential.

## VII. DISCUSSION

In the following discussion, estimates of the magnitude of the  $T$ -violating Hamiltonian will be obtained based on the present results. Such a discussion must of necessity be of a somewhat qualitative nature, as a number of crude estimates are required. However, as we are not interested in determining the exact magnitude of the  $T$ -violating interaction, but rather in distinguishing among order-of-magnitude estimates provided by various theories, such a discussion will suffice for these purposes. As the following calculation is rather phenomenological, we wish to stress the importance of detailed theoretical calculations based on the previously proposed theories of  $T$  violation.

We make the following assumptions: (1) We consider the case in which  $T$  violation occurs in the nuclear Hamiltonian rather than in the electromagnetic radiation field operators discussed in the previous section. There is no sound physical basis for this assumption, and one could easily carry through the discussion including both possible origins of  $T$  violation, yielding finally a comparison between an empirical result and the sum of two terms each associated with one of these two origins of  $T$  violation. One then must, as was for example done by Blin-Stoyle and Coutinho,<sup>10</sup> as-

TABLE III. Summary of experimental studies of  $T$  invariance in  $\gamma$  decay.

| Nucleus           | Method <sup>a</sup> | $\delta$ <sup>b</sup> | $\sin\eta$<br>(Units of $10^{-3}$ ) | $H_w(L)$ <sup>c</sup> | $H_w(L+1)$         | $\text{Im}\langle L \rangle_w$<br>(Upper limits) | $\text{Im}\langle L+1 \rangle_w$<br>(Upper limits) | Ref.         |
|-------------------|---------------------|-----------------------|-------------------------------------|-----------------------|--------------------|--|--|--------------|
| <sup>36</sup> Cl  | $n-\gamma$          | +0.21                 | $0.8 \pm 2.3$                       | (0.26)                | (0.1)              | $6 \times 10^{-3}$                               | $1 \times 10^{-2}$                                 | 3            |
| <sup>49</sup> Tl  | $n-\gamma$          | +0.053                | $17 \pm 25$                         | (21)                  | (0.1)              | $1 \times 10^{-2}$                               | $1 \times 10^{-1}$                                 | 4            |
| <sup>56</sup> Fe  | $\beta-\gamma$      | +0.23                 | $4 \pm 26$                          | (2.5)                 | (0.1)              | $2 \times 10^{-2}$                               | $1 \times 10^{-1}$                                 | 5            |
| <sup>99</sup> Ru  | $M-\bar{\epsilon}$  | -1.6                  | $1.0 \pm 1.7$                       | $6 \times 10^3$       | $2 \times 10^{-2}$ | $4 \times 10^{-5}$                               | $2 \times 10^{-2}$                                 | 6            |
| <sup>106</sup> Pd | $\beta-\gamma$      | +0.21                 | $4 \pm 18$                          | (3.5)                 | (0.1)              | $1 \times 10^{-2}$                               | $6 \times 10^{-2}$                                 | 7            |
| <sup>180</sup> Hf | $\bar{I}-\gamma$    | +5.3                  | $48 \pm 87$                         | $1.3 \times 10^{14}$  | $2 \times 10^9$    | $1 \times 10^{-8}$                               | $3 \times 10^{-6}$                                 | Present work |
| <sup>192</sup> Pt | $\bar{I}-\gamma$    | -2.1                  | $4 \pm 5$                           | $(5 \times 10^2)$     | (0.1)              | $5 \times 10^{-4}$                               | $3 \times 10^{-2}$                                 | 8            |
| <sup>193</sup> Ir | $M-\bar{\epsilon}$  | +0.56                 | $1.1 \pm 3.8$                       | 1100                  | $5 \times 10^{-2}$ | $2 \times 10^{-4}$                               | $3 \times 10^{-2}$                                 | 9            |

<sup>a</sup> Method used to achieve polarization of initial level ( $\beta$ —previous  $\beta$  decay;  $\bar{I}$ —low-temperature orientation;  $M$ —Mössbauer scattering;  $n$ —polarized neutron capture) and to observe final orientation ( $\gamma$ —angular distribution of subsequent  $\gamma$  ray;  $\bar{\epsilon}$ — $\gamma$ -ray linear polarization).

<sup>b</sup>  $E2/M1$ , except  $E3/M2$  for <sup>180</sup>Hf.

<sup>c</sup> Hindrance of  $\gamma$ -ray transition probability relative to Weisskopf estimates; values in parentheses are estimated by assuming the  $E2$  transition to be enhanced by a factor of 10.

sume that the two terms do not cancel and use the empirical result as an estimate of either term. We choose to simplify the ensuing discussion somewhat by considering only the possibility of  $T$  violation in the nuclear Hamiltonian. (We note in passing that Siegert's theorem may be used to eliminate the cancellation problem for electric multipoles only.<sup>10</sup>) (2) We assume the validity of first order perturbation theory for treating the state vectors, and include only one of the possible states which can mix with the unperturbed state. The latter question of which states can mix with the unperturbed states such as to maximize the  $T$ -violating effect is one which requires calculations beyond the scope of this investigation.

The nuclear Hamiltonian may be decomposed into its  $T$ -even (invariant) and  $T$ -odd parts as

$$H = H_{\text{even}} + H_{\text{odd}}, \quad (19)$$

where

$$T^{-1}H_{\text{even}}T = H_{\text{even}}, \quad (20)$$

$$T^{-1}H_{\text{odd}}T = -H_{\text{odd}}, \quad (21)$$

assuming  $\sin\eta$  to be small)

$$\begin{aligned} \frac{|\delta| \sin\eta}{1 + |\delta|^2} \approx & \left\{ \langle 6^+ \| E3 \| 8^- \rangle \left[ -\frac{i^{-1} \langle \tilde{8}^- \| H_{\text{odd}} \| 8^- \rangle}{E_{8^-} - E_{\tilde{8}^-}} \langle 6^+ \| M2 \| \tilde{8}^- \rangle + \frac{i^{-1} \langle \tilde{6}^+ \| H_{\text{odd}} \| 6^+ \rangle}{E_{6^+} - E_{\tilde{6}^+}} \langle 6^+ \| M2 \| 8^- \rangle \right] \right. \\ & \left. - \langle 6^+ \| M2 \| 8^- \rangle \left[ -\frac{i^{-1} \langle \tilde{8}^- \| H_{\text{odd}} \| 8^- \rangle}{E_{8^-} - E_{\tilde{8}^-}} \langle 6^+ \| E3 \| \tilde{8}^- \rangle + \frac{i^{-1} \langle \tilde{6}^+ \| H_{\text{odd}} \| 6^+ \rangle}{E_{6^+} - E_{\tilde{6}^+}} \langle \tilde{6}^+ \| E3 \| 8^- \rangle \right] \right\} \\ & \times [ |\langle 6^+ \| M2 \| 8^- \rangle|^2 + |\langle 6^+ \| E3 \| 8^- \rangle|^2 ]^{-1} \end{aligned} \quad (25)$$

or equivalently,

$$\sin\eta \approx \frac{i \langle \tilde{8}^- \| H_{\text{odd}} \| 8^- \rangle}{E_{8^-} - E_{\tilde{8}^-}} \left[ \frac{\langle 6^+ \| M2 \| \tilde{8}^- \rangle}{\langle 6^+ \| M2 \| 8^- \rangle} - \frac{\langle 6^+ \| E3 \| \tilde{8}^- \rangle}{\langle 6^+ \| E3 \| 8^- \rangle} \right] + \frac{i \langle \tilde{6}^+ \| H_{\text{odd}} \| 6^+ \rangle}{E_{6^+} - E_{\tilde{6}^+}} \left[ -\frac{\langle \tilde{6}^+ \| M2 \| 8^- \rangle}{\langle 6^+ \| M2 \| 8^- \rangle} + \frac{\langle \tilde{6}^+ \| E3 \| 8^- \rangle}{\langle 6^+ \| E3 \| 8^- \rangle} \right]. \quad (26)$$

Here we have considered out-of-phase admixtures to both the  $6^+$  and  $8^-$  levels, and we have dropped the subscript "even" with the understanding that state vectors without the tilde are taken to be  $T$  even (i.e., unperturbed). In Eq. (26), the  $\gamma$ -ray matrix elements are all real, since the complex phase has been incorporated by means of the matrix elements of  $H_{\text{odd}}$ , which are purely imaginary.

It should be noted that both the matrix elements of  $H_{\text{odd}}$  and the  $\gamma$ -ray matrix elements connecting  $T$ -odd with  $T$ -even states are pure imaginary; the former follows from the properties of  $H_{\text{odd}}$  under  $T$ , Eq. (21), while the latter is a general characteristic of the electromagnetic multipole moments and is independent of the phase convention used (see for example the discussion by Steffen and Alder).<sup>32</sup>

The  $\gamma$ -ray matrix element ratios may be estimated from the systematics of  $\gamma$ -ray hindrances

with  $T$  being the operator of the time-reversal symmetry ( $t \rightarrow -t$ ). Under the assumption of  $T$  invariance, the phases of the state vectors are defined in a consistent way, such as

$$T |Im\rangle = (-1)^{I-m} |I-m\rangle, \quad (22)$$

but under  $H_{\text{odd}}$  that is no longer possible, and the perturbed state vector becomes

$$|I\rangle = |I\rangle_{\text{even}} + i\epsilon |I\rangle_{\text{odd}}. \quad (23)$$

Here the complex phase is written explicitly such that  $\epsilon$  is real. This may be written as

$$|I\rangle = |I\rangle_{\text{even}} + \sum_{\tilde{I} \neq I} \frac{\langle \tilde{I} \| H_{\text{odd}} \| I \rangle_{\text{even}}}{E_I - E_{\tilde{I}}} |\tilde{I}\rangle, \quad (24)$$

where the sum is carried out over all states  $\tilde{I}$  of the same angular momentum as  $I$  (except the unperturbed state). We consider only a single state  $\tilde{I}$ , dropping the summation, and following a procedure similar to that of Ref. 12, we obtain (again

with respect to  $\Delta K$ , as tabulated by Löbner.<sup>33</sup> We wish to maximize the  $\gamma$ -ray matrix elements of the various numerators of Eq. (26), and hence it is desirable to admix collective states, which characteristically show enhanced  $\gamma$ -ray transition probability. Conversely, the matrix elements of  $H_{\text{odd}}$  will probably be small for collective states, but may be particularly large for states differing by two quasiparticles from the unperturbed state.<sup>15</sup> A number of low-lying, high- $K$  two quasiparticle states is available in  $^{180}\text{Hf}$ ,<sup>34</sup> but the  $\gamma$ -ray branchings are such that none is expected to have particularly large  $\gamma$ -ray matrix elements connecting with the appropriate levels. We thus choose to admix collective states, in particular the  $K=2$   $\gamma$  vibration into the  $6^+$  state and  $K=2$  or  $K=3$  octupole vibrations into the  $8^-$  state. We assume that such a choice does not result in too great a reduction in the matrix elements of  $H_{\text{odd}}$ , since the collec-

tive state may be treated as a coherent superposition of quasiparticle pairs, (i.e., as the lowest-lying random-phase-approximation state) with at least some of the paired states having reasonably large matrix elements of  $H_{\text{odd}}$  with the unperturbed states. The matrix element ratios may then be expressed as ratios of Weisskopf hindrances, with  $M_w$  indicating the appropriate Weisskopf estimate for the matrix element:

$$\frac{\langle 6^+ \| M2 \| \bar{8}^- \rangle}{\langle 6^+ \| M2 \| 8^- \rangle} = \frac{2 \times 10^{-2} M_w(M2)}{0.8 \times 10^{-7} M_w(M2)} = 2.5 \times 10^5, \quad (27a)$$

$$\frac{\langle 6^+ \| E3 \| \bar{8}^- \rangle}{\langle 6^+ \| E3 \| 8^- \rangle} = \frac{3 M_w(E3)}{2 \times 10^{-5} M_w(E3)} = 1.5 \times 10^5, \quad (27b)$$

$$\frac{\langle \bar{6}^+ \| M2 \| 8^- \rangle}{\langle 6^+ \| M2 \| 8^- \rangle} = \frac{10^{-4} M_w(M2)}{0.8 \times 10^{-7} M_w(M2)} = 1.2 \times 10^3, \quad (27c)$$

$$\frac{\langle \bar{6}^+ \| E3 \| 8^- \rangle}{\langle 6^+ \| E3 \| 8^- \rangle} = \frac{10^{-3} M_w(E3)}{2 \times 10^{-5} M_w(E3)} = 5 \times 10^1. \quad (27d)$$

The hindrances of the electromagnetic matrix elements connecting the  $T$ -odd and  $T$ -even states have been estimated from the compilation of Löbner,<sup>33</sup> assuming the  $\bar{6}^+$  state to be  $K=2$  and the  $\bar{8}^-$  state to be  $K=2$  or  $K=3$ . On the basis of the magnitudes of the transition matrix elements, the second term of Eq. (26) may be neglected; further, the negative sign appearing in the quantity in brackets of the first term is meaningless unless we know the relative phases of the  $T$ -odd  $\gamma$ -ray matrix elements. Since this sign is unknown, we estimate the bracket at  $2 \times 10^5$ . Assuming the octupole band head to be at 1.5 MeV, the energy difference in the denominator is estimated to be 1.5 MeV, and hence

$$|\langle \bar{8}^- | H_{\text{odd}} | 8^- \rangle| \approx \sin \eta \frac{1.5 \text{ MeV}}{2 \times 10^5}. \quad (28)$$

Using the present value for  $\sin \eta$ , we obtain:

$$|\langle \bar{8}^- | H_{\text{odd}} | 8^- \rangle| \approx 0.4 \pm 0.7 \text{ eV}. \quad (29)$$

This may be compared with the value  $90 \pm 110 \text{ eV}$  deduced by Blin-Stoyle and Coutinho<sup>10</sup> in  $^{192}\text{Pt}$ ; the smaller upper limit in the present case results entirely from the large hindrance of the transition studied in the present work.

An interpretation of the above result in terms of suggested  $T$ -odd potentials is difficult, owing to the lack of information on the form of such potentials. The general forms of  $T$ -odd single-particle and nucleon-nucleon potentials have been suggested by Herczeg,<sup>35</sup> and Huffman<sup>36</sup> has indicated the form of  $T$ -violating potentials originating in the electromagnetic interaction. Clement<sup>15</sup> has discussed  $T$ -violating potentials based on two-nucleon electromagnetic transition operators (real

photons) and also on three-nucleon potentials corresponding to the exchange of virtual photons. Once a specific form of the potential is assumed, it is then necessary to evaluate the matrix elements of that potential between the nuclear state of interest (in the present case, the  $8^-$  level of  $^{180}\text{Hf}$  at 1142 keV) and other states which might be admixed by  $H_{\text{odd}}$ . It is probable that simple potentials such as those of the single-particle type are likely to have strongly inhibited matrix elements between the low-lying levels; for example, a potential of the form  $\vec{r} \cdot \vec{p}$  has matrix elements between states  $A$  and  $B$  proportional to  $(E_A - E_B) \times \langle A | r | B \rangle$ , and the matrix elements of the operator  $r$  between the low-lying levels may be inferred (from the systematics of  $E1$  transition moments compiled by Löbner<sup>33</sup>) to be retarded by at least a factor of  $10^3$ . On the other hand, while more sophisticated potentials involving additional momentum-dependent terms might not suffer from this inhibition, such additional terms are intrinsically smaller due to the small nucleon momenta involved ( $v/c < 0.1$ ). It seems safe to assume that effects of this sort contribute a reduction of at most  $10^2 - 10^3$  to the matrix elements of  $H_{\text{odd}}$ , and thus we may conclude that the "intrinsic" magnitude of  $H_{\text{odd}}$ , excluding nuclear structure effects, is at most 1 keV. This estimate is considerably smaller than the energies normally associated with the strong (100 MeV) or electromagnetic (1 MeV) interactions, suggesting that the source of any  $T$  violation may lie elsewhere.

## VIII. CONCLUSIONS

Based on considerations involving effects of possible  $T$ -violating internucleon interactions, an upper limit on any observable effect in  $^{180}\text{Hf}$  associated with  $T$  violation in nuclei has been shown to be sufficiently small to suggest that  $T$  violation is unlikely to arise from the strong or electromagnetic interactions. Definitive conclusions regarding the source of  $T$  violation require calculations, based on more realistic potentials, beyond the scope of the present work. However, the above considerations demonstrate clearly the advantages of using strongly hindered  $\gamma$  transitions to obtain a relative amplification of small effects in nuclear interactions.

## ACKNOWLEDGMENTS

We wish to acknowledge the participation of C. E. Olsen in the experimental work, particularly the (Hf, Zr)Fe<sub>2</sub> preparation. Our thanks are also extended to Peter Herczeg for many useful discussions. One of us (B.T.M.) expresses gratitude for the financial support of Associated Western Universities, Inc. and for the hospitality of the Los Alamos Scientific Laboratory.

- <sup>†</sup>Work performed under the auspices of the U.S. Atomic Energy Commission.
- \*U.S. Atomic Energy Commission-Associated Western Universities, Inc. Fellow. Permanent address: Physics Department, Utah State University, Logan, Utah 84321.
- <sup>1</sup>E. M. Henley, *Annu. Rev. Nucl. Sci.* **19**, 367 (1969).
- <sup>2</sup>J. H. Christenson, J. W. Cronin, V. L. Fitch, and R. Turlay, *Phys. Rev. Lett.* **13**, 138 (1964).
- <sup>3</sup>J. Eichler, *Nucl. Phys.* **A120**, 535 (1968).
- <sup>4</sup>J. Kajfosz, J. Kopecky, and J. Honzatko, *Nucl. Phys.* **A120**, 225 (1968).
- <sup>5</sup>M. Garrell, H. Frauenfelder, D. Ganek, and D. C. Sutton, *Phys. Rev.* **187**, 1410 (1969).
- <sup>6</sup>O. C. Kistner, *Phys. Rev. Lett.* **19**, 872 (1967).
- <sup>7</sup>R. B. Perkins and E. K. Ritter, *Phys. Rev.* **174**, 1426 (1968).
- <sup>8</sup>M. J. Holmes, W. D. Hamilton, and R. A. Fox, *Nucl. Phys.* **A199**, 401 (1973).
- <sup>9</sup>M. Atac, B. Chrisman, P. Debrunner, and H. Frauenfelder, *Phys. Rev. Lett.* **20**, 691 (1968).
- <sup>10</sup>R. J. Blin-Stoyle and F. A. Bezerra Coutinho, *Nucl. Phys.* **A211**, 157 (1973).
- <sup>11</sup>R. J. Blin-Stoyle, *Fundamental Interactions and the Nucleus* (North-Holland, Amsterdam, 1973), Chap. 1.
- <sup>12</sup>W. A. Steyert and K. S. Krane, *Phys. Lett.* **47B**, 294 (1973). We note a sign error in Eq. (4) of this reference.
- <sup>13</sup>B. Jenschke and P. Bock, *Phys. Lett.* **31B**, 65 (1970); E. D. Lipson, F. Boehm, and J. C. Vanderleeden, *ibid.* **35B**, 307 (1971).
- <sup>14</sup>K. S. Krane, C. E. Olsen, J. R. Sites, and W. A. Steyert, *Phys. Rev. C* **4**, 1906 (1971).
- <sup>15</sup>C. F. Clement and L. Heller, *Phys. Rev. Lett.* **27**, 545 (1971); C. F. Clement, *Ann. Phys. (N. Y.)* **75**, 219 (1973).
- <sup>16</sup>A. Barroso and R. J. Blin-Stoyle, *Phys. Lett.* **45B**, 178 (1973).
- <sup>17</sup>B. T. Murdoch, C. E. Olsen, W. A. Steyert, and K. S. Krane, *Phys. Rev. Lett.* **31**, 1514 (1973).
- <sup>18</sup>C. M. Lederer, J. M. Hollander, and I. Perlman, *Table of Isotopes* (Wiley, New York, 1967).
- <sup>19</sup>H. J. Körner, F. E. Wagner, and B. D. Dunlap, *Phys. Rev. Lett.* **27**, 1593 (1971).
- <sup>20</sup>E. Bodenstedt, H. J. Körner, E. Gerdau, J. Radeloff, C. Günther, and G. Strube, *Z. Phys.* **165**, 57 (1961).
- <sup>21</sup>B. A. Jacobsohn and E. M. Henley, *Phys. Rev.* **113**, 234 (1959).
- <sup>22</sup>F. Boehm, in *Hyperfine Structure and Nuclear Radiations*, edited by E. Matthias and D. A. Shirley (North-Holland, Amsterdam, 1968), p. 279.
- <sup>23</sup>K. S. Krane, R. M. Steffen, and R. M. Wheeler, *Nucl. Data* **A11**, 351 (1973).
- <sup>24</sup>K. S. Krane and R. M. Steffen, *Phys. Rev. C* **2**, 724 (1970).
- <sup>25</sup>K. S. Krane, University of California Lawrence Berkeley Laboratory Report No. LBL-1686 (unpublished).
- <sup>26</sup>R. M. Steffen and H. Frauenfelder, in *Perturbed Angular Correlations*, edited by E. Karlsson, E. Matthias, and K. Siegbahn (North-Holland, Amsterdam, 1964), Chap. 1.
- <sup>27</sup>V. S. Shirley, in *Hyperfine Interactions in Excited Nuclei*, edited by G. Goldring and R. Kalish (Gordon and Breach, New York, 1971), p. 1255.
- <sup>28</sup>Supercon, Inc., 9 Erie Drive, Natick, Massachusetts 01760.
- <sup>29</sup>K. S. Krane, J. R. Sites, and W. A. Steyert, *Rev. Sci. Instrum.* **42**, 1475 (1971).
- <sup>30</sup>Data General Corporation, Southboro, Massachusetts 01722.
- <sup>31</sup>L. E. Handy and W. A. Steyert, *IEEE Trans. Nucl. Sci.* (to be published).
- <sup>32</sup>R. M. Steffen and K. Alder, in *The Electromagnetic Interaction in Nuclear Physics*, edited by W. D. Hamilton (North-Holland, Amsterdam, to be published).
- <sup>33</sup>K. E. G. Löbner, *Phys. Lett.* **26B**, 369 (1968).
- <sup>34</sup>J. I. Zaitz and R. K. Sheline, *Phys. Rev. C* **6**, 506 (1972).
- <sup>35</sup>P. Herczeg, *Nucl. Phys.* **75**, 655 (1966).
- <sup>36</sup>A. H. Huffman, *Phys. Rev. D* **1**, 882 (1970).